Int. J. Morphol.,
42(3):718-727, 2024.

Histological and Ultrastructural Changes in Lungs One Year Post Asymptomatic or Mild SARS-CoV-2 Infection: Evaluating the Potential for Active Virus Presence

Cambios Histológicos y Ultraestructurales en los Pulmones un Año Después de una Infección Asintomática o Leve por SARS-CoV-2: Evaluación del Potencial de Presencia Activa del Virus

Elif Kervancioglu Demirci[1]; Engin Alp Onen[2]; Erva Sevic Yilmaz[1]; Hasan Serdar Mutlu[3] & Zuleyha Bingol[4]

KERVANCIOGLU DEMIRCI, E.; ONEN, E. A.; YILMAZ, E. S.; MUTLU, H. S. & BINGOL, Z. Histological and ultrastructural changes in lungs one year post asymptomatic or mild SARS-CoV-2 infection: Evaluating the potential for active virus presence. *Int. J. Morphol., 42(3)*:718-727, 2024.

SUMMARY: Prior research on post-COVID-19 or long COVID primarily focused on the presence of SARS-CoV-2 mostly in symptomatic patients. This study aimed to investigate the persistence of SARS-CoV-2 after 1 year of asymptomatic or mild COVID-19. SARS-CoV-2 infected and control K18-hACE2 transgenic mice (n=25) were studied. Moderate and severe symptomatic subjects were sacrificed after eight days, while mild or asymptomatic mice were kept in BSL-III for twelve months. Analyses included general condition, histochemistry, immunohistochemistry, transmission electron microscopy, and qRT-PCR. Lungs from the twelve-month group showed thickening of alveolar walls, with some lungs exhibiting the recruitment of inflammatory cells, the presence of SARS-CoV-2 mRNA, immunopositivity for the SARS-CoV-2 spike protein, and TEM showed viruses (60-125 nm) within vesicles, indicating continued replication. Certain lung samples showed persistent SARS-CoV-2 presence in Club cells, endothelial cells, and macrophages. The eight-day group exhibited viral interstitial pneumonitis, SARS-CoV-2 immunopositivity, and mRNA. The eight-day hearts displayed viral mRNA, while the twelve-month hearts tested negative. Some asymptomatic twelve-month subjects presented reduced surfactant, basal membrane thickening, fibrosis, and mild autonomic nerve degeneration. In this study conducted on mice, findings indicate the potential for chronic persistence of SARS-CoV-2 in the lungs one year post initial mild or asymptomatic infection, which could suggest the possibility of recurrent episodes in similar human conditions. The observed thickening of alveolar walls and potential fibrotic areas in these mice may imply an increased risk of post-COVID fibrosis in humans. Furthermore, the presence of SARS-CoV-2-positive inflammatory cells in some asymptomatic murine cases could herald a progression toward ongoing inflammation and chronic lung disease in humans. Therefore, the necessity for further studies in human subjects and vigilant monitoring of high-risk human populations is underscored.

KEY WORDS: Asymptomatic; Fibrosis; Electron microscopy; Post-Acute COVID-19 Syndrome; Tuberculosis.

INTRODUCTION

A series of researchers have highlighted the presence of Severe acute respiratory syndrome coronavirus 2 (SARS-CoV-2) during the convalescent phase of infection. While some studies have shown the persistence of the virus for a few months after recovery, no study has reported the presence of viral antigens in the lungs at twelve months following mild and asymptomatic Coronavirus disease 2019 (COVID-19) infection (Cheung *et al*., 2022; Goh *et al*., 2022; Kervancioglu Demirci *et al*., 2023).

The long-term effects of asymptomatic SARS-CoV-2 are still not fully understood, including the possibility of viral persistence, relapse, transmission, reinfection, and chronic damage such as post-viral fibrosis or chronic lung disease.

SARS-CoV-2 enters cells through the angiotensin-converting enzyme-2 (ACE2) receptor, triggering the renin-angiotensin system and causing increased angiotensin II

[1] Histology and Embryology Department, Istanbul Faculty of Medicine, Istanbul University, Istanbul, Turkey.
[2] Vaccine and Biotechnology R&D, Kocak Pharmaceuticals, Tekirdag, Turkey.
[3] Histology and Embryology Department, Faculty of Medicine, Giresun University, Giresun, Turkey.
[4] Pulmonary Medicine Department, Istanbul Faculty of Medicine, Istanbul University, Istanbul, Turkey.
FUNDING. This study was funded by Scientific Research Projects Coordination Unit of Istanbul University (Project number: TAB2021-37258).

Received: 2023-12-21 Accepted: 2024-02-10

levels, leading to severe vasculopathy, coagulopathy, and inflammation with increased monocyte activity is a significant contributor to inflammation in severe SARS-CoV-2 cases (Merad & Martin, 2020; Miesbach, 2020). Utilizing human ACE2 expressing K18-hACE2 transgenic mice, originally developed for studying SARS-CoV infection, allows for the isolated examination of the virus's effects, independent of comorbidities and drug influences, throughout the study period (Moreau *et al*., 2020).

This study aimed to assess lung morphology and viral status in mild symptomatic or asymptomatic K18-hACE2 transgenic mice exposed to single dose SARS-CoV-2 inhalation after one year, comparing the results with control subjects and mice with acute infection.

MATERIAL AND METHOD

Animals. A SARS-CoV-2 alpha strain (Vial no. 31242/12.05.2020), originally isolated from bronchoalveolar lavage specimens and throat swabs from a hospitalized patient and provided by the Turkish Ministry of Health, was subsequently cultured using Vero CCL-81 cells and amplified for the virus bank (Alp Onen *et al*., 2022). All experimental protocols were conducted in BSL-III cabinets in accordance with the Guide for the Care and Use of Laboratory Animals published by the Ministry of Science and Technology. The study received approval from the appropriate ethics committee (Ethical Review Board Name: KODEHAL Animal Care and Use Committee Date: 05.11.2021 Number: KOHADYEK 2021-10). All surgeries were conducted using ketamine-xylazine anesthesia, with utmost care taken to minimize any suffering.

Twenty-five 8-9-week-old male K18-hACE2 on BALB/cJ mice (the Jackson Laboratory, Maine, USA), were divided randomly into control (n=5, without viral exposure) and infected groups (n=20). And were kept in IVC cages (22°C, 55-65 % relative humidity). After a dose of intranasal 104 TCID50 live viruses SARS-CoV-2 was administered into both nasal passages using a micropipette in an isolator cabinet (220 Pa negative pressures), severe and moderately symptomatic mice were euthanized by or until the 8th day (n=10, eight-day group), while the remaining mild and asymptomatic mice were kept for a duration of 12 months (n=10, twelve-month group) (Alp Onen *et al*., 2022) (Supplementary file, S1).

Control mice showed no symptoms during the experiment. Six mice were sacrificed at the fourth, fifth, sixth, and seventh days due to severe infection and symptoms of lethargy. Additionally, four mice that had lost weight due to moderate or severe infection were sacrificed at the eighth day. This group of ten mice was considered as eight-day group. The remaining ten infected mice of little or no weight loss, mild or no symptoms recovered and were fed ad libitum for twelve months.

To assess the clinical condition, daily activity scores and weight loss were recorded. For weight loss, the difference between day zero and day eight was calculated as the percentage of change with the formula: % of change = -(Initial weight–Weight at 8th day or the last day alive) / Initial weight x 100. For clinical progression, daily monitoring was performed by blinded investigators and recorded using a grading system modified from the literature (van Griensven *et al*., 2002; Moreau *et al*., 2020) (Supplementary file, S1).

Histopathological examinations of lungs. Tissues were fixed in neutral buffered formalin for at least 24 hours. Manual processing included washing in tap water and graded series of ethanol (70 %, 90 %, 96 %, 100 %), toluene, and paraffin. Lung sections of five µm thickness (Leica RM22555, Wetzlar, Germany) were stained with Hematoxylin and Eosin, as well as Masson's trichrome stain. Histological examination and fibrosis assessment were performed using the Modified Ashcroft scale (Supplementary file, S2) (Hübner *et al*., 2008). Two histologists, blinded to the study groups, made the observations with a light microscope (Leica DMLB, Wetzlar, Germany). The whole section area was observed at x20 magnification, and mean grade scores of all visible areas were recorded. Grade ranged from zero to eight, representing normal lung to total obliteration.

SARS-CoV-2 detection by immunohistochemistry of lungs. The tissue sections were treated with 3 % hydrogen peroxidase to prevent endogenous peroxidase activity. Antigenic structures were released using citrate buffer (pH: 6.0) with heat. Overnight incubation at 4°C was done with anti-SARS-CoV-2 Spike Glycoprotein antibody (ab275759, ABCAM, Cambridge, UK) at a 1:500 dilution. HRP anti-polyvalent kit (Ultravision, ThermoFischer Scientific, Massachusetts, USA) was used for secondary antibody and peroxidase applications. AEC (Labvision, ThermoFischer Scientific, Massachusetts, USA) was selected as the chromogen. Counterstaining with Hematoxylin was performed. Immunohistochemical stainings were validated using positive and negative controls (Supplementary file, S3).

Real-Time PCR of Lungs and Hearts. For quantitative real-time PCR analysis, lung and heart samples were homogenized with proteinase K (Roche, Germany) in the control group (n=4), the eight-day group (n=4), and the twelve-month group (n=5) mice. Viral nucleic acids were extracted using the Viral Nucleic Acid Kit (Roche, Germany).

A one-step qRT-PCR kit (Primer Design, USA) designed for quantitative detection of SARS-CoV-2 RNA-dependent RNA polymerase (RdRp) was used for reverse transcriptase polymerase chain reaction (RT-PCR). Amplification was performed on a LightCycler 480 real-time PCR instrument (Roche, Germany) following manufacturer recommendations, with the viral load automatically calculated based on the standard curve using the instrument's software.

The one-step real-time RT-PCR technology of the One-Step RT-PCR Kit (Primer Design, USA) allowed qualitative determination of specific RNA. This kit can detect the virus at different loads, ranging from 2 x 10^0 to 2 x 10^5 copies per reaction, covering both low and high viral loads and enabling detection at various stages of infection.

Transmission Electron Microscopy of Lungs. For transmission electron microscopy (TEM), 1mm sized samples were fixed for four hours in 2,5 % gluteraldehyde in 0.1 M phosphate buffer (pH 7.4) and one hour in 2 % osmium tetroxide in phosphate buffer at room temperature. After a graded ethanol series (50 %, 75 %, 96 %, 100 %, 100 %) and propylene oxide, tissues were embedded in epoxy resin (Epon 812, Sigma, USA). Thin sections of 90 nm were contrasted with uranyl acetate and lead citrate and photographed using a transmission electron microscope (Jeol, Tokyo, Japan). Two specialized histologists made the observations.

Statistical analysis. The statistical analysis was conducted with GraphPad Prism 9.4.0 (GraphPad Software, San Diego, CA, USA). To assess normality, the Shapiro-Wilk test was used. The percentage change in weight, modified Ashcroft scores, and qRT-PCR values exhibited normal distribution, and these data, represented as means ± standard error of the mean (SEM) in column bar graphs, were subjected to analysis of variance (ANOVA) with subsequent Tukey's multiple comparison tests. Statistical significance was defined as a p-value less than 0.05.

RESULTS

Clinical assessment of animals. SARS-CoV-2 infected mice showed reduced activity and decreased food intake within days were considered to have severe or moderate illness and were included in the eight-day group. These subjects exhibited significant weight loss (5.578 ± 1.555 %). The weight percent change in the eight-day group was significantly different from that of the control group and the twelve-month group (P=0.0018 and P<0.0001, respectively) (Fig. 1).

The SARS-CoV-2 infected remaining subjects without any symptoms and with consistent adequate responses to the environment, slight interruptions in activity, slightly decreased food intake, or virus inhaled mice with no symptoms were considered mildly ill and asymptomatic subjects. These subjects were chosen for the twelve-month group. These subjects weight loss percent changes in the first week were nonsignificant, and their activity score raised to five in the following days and weeks (Supplementary file, S1).

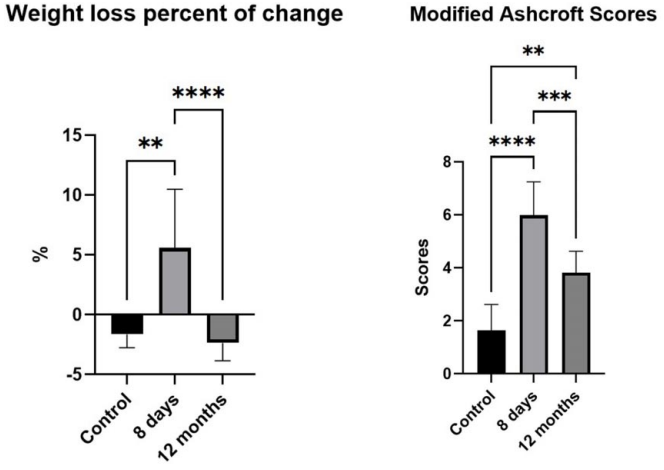

	Applied Measure	Control	8 days	12 months
a	Activity score	5, 5, 5, 4, 5	0, 0, 2, 0, 0, 0, 3, 0, 3, 2	4, 4, 4, 4, 4, 5, 4, 4, 4, 5
b	Weight loss percent of change	-0.1, -2.5, -0.7, -2.3, -2.4	9.9, 4, 1.9, 10, 8.3, 10.4, -0.2, 11.2, 0.3, -0.4	-3.4, -2.5, 0.1, -1.1, -3.7, -4.3, -2.5, -1.6, -0.5, -3.6
c	Modified Ashcroft Scores	1,646±0.3429	5,990±0,3993	3,816±0,2872

Fig. 1. The clinical assessment and histopathological scoring of the animals. The weight loss percent of change and Modified Ashcroft Scores were drawn in graphs. a. Activity scores showed the general condition of animals on the 8th day of the experiment. b. The weight loss percent of change at the 8th day for all the groups represented a significant difference between groups. For early sacrificed animals, the last measured weight was recorded. Weight loss data for each animal was listed in this figure with one decimal and calculated with 6 decimals. c. The mean ± SEM data of the modified Ashcroft scores of lung tissues in the eight-day vs. twelve-month were statistically different. **, P<0.01; ***, P<0.001; ****, P<0.0001.

The control group subjects were normal in activity. They were strong, curious, had quick movements, normal food intake, and sometimes only occasional interruptions in activity. They did not lose weight during the period of the experiment.

Histopathological Examination. In the twelve-month group, thickening of alveolar walls was observed in all lungs. In some of the samples, bronchioles showed mild cellular debris, along with an excess of lymphomonocytic cells in vessels and occasional lymphoid infiltrations around them. The connective tissue surrounding bronchioles appeared thicker, and congestion was noted in some large vessels (Fig. 2).

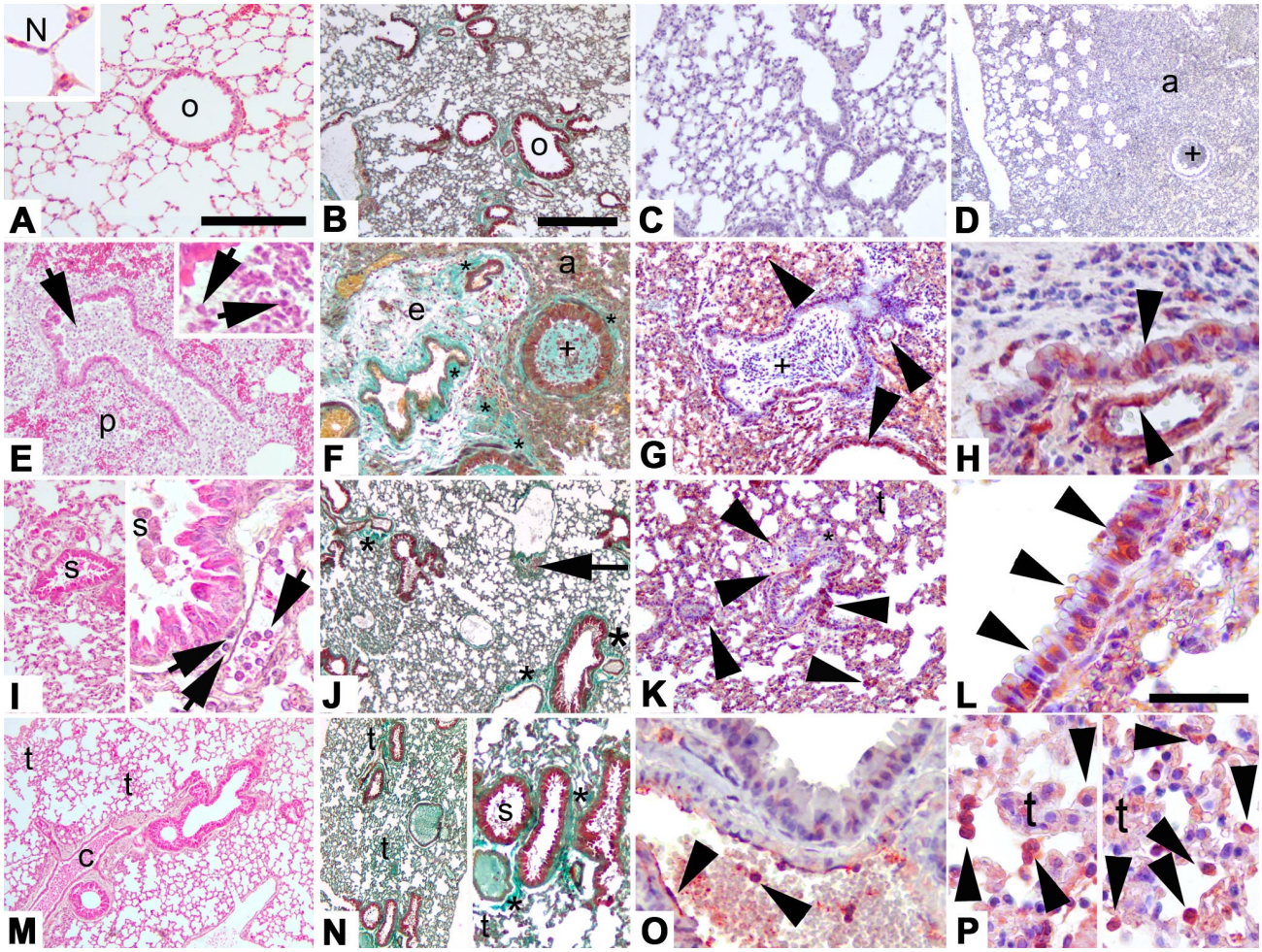

Fig. 2. Light microscopic evaluations. A, A inset & B. The control group had normal lung parenchyma, thin alveolar septa (N) (thin to max <3x thickened), erythrocytes in capillaries, and intact bronchioles (o). C. The control group was negative for SARS-CoV-2 spike protein. D. Negative control of a sample from the eight-day group with non-immune serum. E & E inset. The eight-day group showed interstitial pneumonitis (p), and some of the bronchioles were dilated and obstructed (+) with mucus, cellular debris, and inflammatory cells (short arrow). F. Alveolar walls were filled with exudation (e) and extravasated cells (a), alveolar air spaces were narrowed, perivascular, alveolar septal, and peribronchial fibrosis (asterisk) were observed. G and H. Club cells and endothelium were positive for SARS-CoV-2 (arrowhead), and the type II pneumocytes were moderately stained. I, J, M, N. In the 12 months after infection group, alveolar septa were thickened (t) more than three times normal with patchy small fibrotic masses in some areas. Bronchiolar lumen had cellular debris. The interstitial area and neighboring blood vessels contained lymphomonocytic cells indicating continuing inflammatory injury. Some large blood vessels were congested (c). J&N. Peribronchial fibrosis (*) was present. The bronchiolar lumen had cellular debris (s), and lymphoid infiltration was near a large blood vessel (long arrow). K, L, O, P. SARS-CoV-2 positivity was high in lymphomonocytic cells in blood vessels, endothelial cells, and macrophages in the alveolar lumen, moderate in Club cells, and low in Type II pneumocytes. A, E, I, M: Hematoxylin-eosin staining; B, F, J, N left & right: Masson's trichrome staining; C, D, G, H, K, L, O, P: SARS-CoV-2 spike protein immunostaining. A-C: the control group; D-H: the eight-day group; I-P: the twelve-month group. H, L, O, and P left & right 40X, B, C, D & N left – 4X; all other A-N right are 10X. N right is 10X magnification of N left. H is 40X magnification of G. Scale bars represent 400 µm for 4X, 200 µm for 10X, and 50 µm for 40X.

In the eight-day group, inflammatory cells invaded alveoli. Some bronchioles exhibited dilation and were filled with debris, inflammatory cells, and mucus. In the subjects sacrificed early due to severe illness, the lung structure was retained, but inflamed alveolar walls, occluded air spaces due to extravasated inflammatory cells and erythrocytes, and signs of edema and early fibrosis around bronchioles, blood vessels, and some alveolar walls were observed. Interstitial pneumonitis was commonly observed in this group.

The control group exhibited normal lung parenchyma and intact bronchioles.

There was a statistically significant difference in fibrosis between the groups ($P<0.0001$). The eight-day group showed variable alveolar morphology with patchy affected areas (Control group vs. eight-day group, $P<0.0001$). The twelve-month group displayed predominantly contiguous fibrotic walls. Thickened alveolar septa, measuring more than three times the normal thickness, were observed in all subjects in this group, along with small localized fibrotic areas (Control group vs. twelve-month group, $P=0.0012$ and eight-day group vs. twelve-month group, $P=0.0007$) (Fig. 1).

SARS-CoV-2 spike protein detection by Immunohistochemistry. The eight-day group exhibited immunoreactivity for SARS-CoV-2 in Club cells, type II pneumocytes, and endothelial cells. The staining pattern was consistent with the patchy characteristic of SARS-CoV-2.

In the twelve-month group, most of the lungs showed positivity for SARS-CoV-2 (7/10). Immunohistochemistry revealed SARS-CoV-2 positivity in the alveolar walls and lymphomonocytic cells (7 out of 10 samples). Lymphomonocytic cells in alveolar air spaces and vessels displayed a high staining intensity, similar to endothelial cells. The staining intensity of fibroblasts and type II pneumocytes in these lungs was moderate. Three of the lungs also exhibited continued immunoreactivity in Club cells of bronchioles (Fig. 2).

The lungs of the control group tested negative for SARS-CoV-2 spike antigen.

SARS-CoV-2 mRNA detection by Quantitative Real-Time PCR. In the eight-day group, all four lung samples exhibited a high viral load (Mean 7,10 log 100 number of copies/μl), while all heart samples from the same group displayed a moderate viral load (Mean 4,45 log 100 number of copies/μl).

Lung samples from the twelve-month group yielded both positive and negative PCR results. Two out of five samples tested positive for SARS-CoV-2 mRNA (2,01 log 101 and 2,24 log 101 number of copies/μl), while the remaining three samples were negative (Mean of the group is 9,15 log 10^{-1} number of copies/μl). The heart samples from the twelve-month group (none out of 5) tested negative for SARS-CoV-2 (Mean 1,36 log 10^{-1} number of copies/μl).

Both the lungs and hearts of the control group tested negative for SARS-CoV-2 mRNA (Mean 1,08 log 10^{-1} and 3,71 log 10^{-1}, respectively).

Ultrastructural Examination and SARS-CoV-2 detection by TEM. TEM revealed viruses ranging in size from 65-110 nm in various cell types of the eight-day and twelve-month groups. Both groups exhibited different and similar ultrastructural pathologies at different levels.

In the eight-day group, some specimens exhibited vesicles containing SARS-CoV-2 in Club cells, while free virus-like particles were detected in endothelial cells. Apoptotic cells were widespread in bronchioles, and some cells had desquamated into the lumen. Macrophages had filled some alveolar spaces. In the preserved areas, most of the type II pneumocytes were small and young, with some showing signs of apoptosis. A significant reduction in surfactant content was observed in all of the type II pneumocytes. The basal membrane appeared irregular and thickened in certain areas. Autonomic nerves showed signs of damage, such as splitting myelin lamellas (Fig. 3).

In the twelve-month group, transmission electron microscopy (TEM) confirmed the presence of viruses in some of the specimens. Vesicles filled with viruses were observed in type II pneumocytes and endothelial cells. Free virus-like particles were found in interstitial cells. Viruses were observed on both sides of the basal membrane. Bronchioles exhibited subnormal morphology, with Club cells displaying increased exocytotic activity. Some of the type II pneumocytes showed a reduced amount of surfactant and displayed damaged morphology. Protrusion of type II pneumocytes into the lumen was a common observation. The parenchymal cellularity was elevated, and airspaces appeared narrowed. More capillaries and platelets were visible in microscopic fields. The thickening of the basal membrane was widespread in this group. Mild damage to myelinated autonomic nerves was observed (Fig. 4).

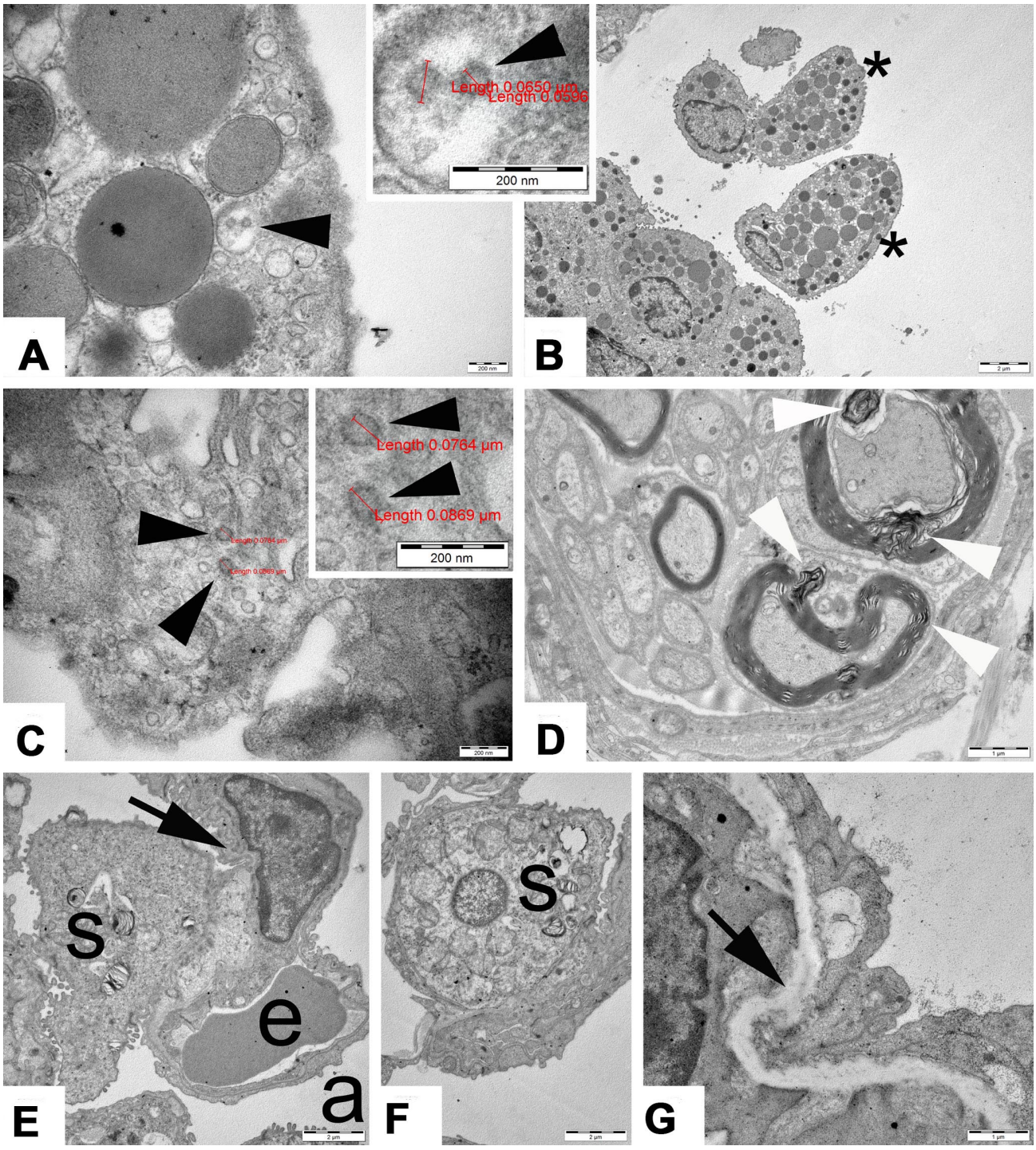

Fig. 3. Transmission electron micrographs of the eight-day group. A&B. Club cells contained approximately 65 nm-sized viruses (black arrowhead) in vesicles and desquamated (*) into the lumen. C. Virus-like particles of approximately 80 nm in size were seen in endothelial cells. D. Myelin sheath lamellae of autonomic nerves were split (white arrowhead). E & F. Most of the type II pneumocytes were young and had a decreased count of surfactant (s). Erythrocytes (e) filled capillaries. G. Basal membrane of the blood-air barrier was thickened (arrow) in some areas. A: 50,000X; A inset (OM): 50,000X; B: 60,000X; C: 60,000X; C inset (OM): 60,000X; D&G: 15,000X; E&F: 7,500X. OM = optically magnified.

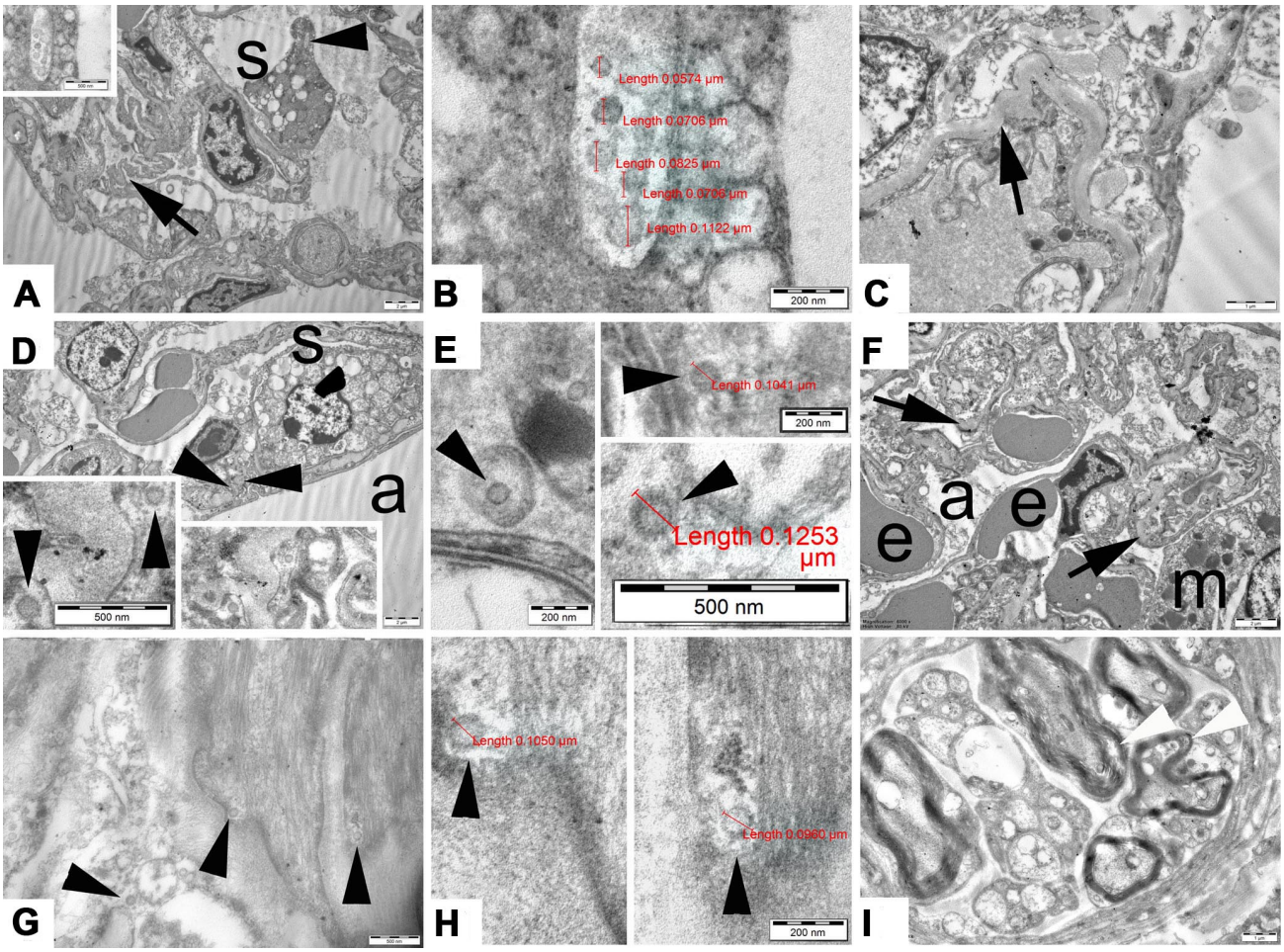

Fig. 4. Transmission electron micrographs of the twelve-month group. A, A inset & B. A vesicle filled with 60-110 nm viruses (black arrowhead) was seen in a type ıı pneumocyte, which had reduced surfactant (s). C. The basal membrane of the blood-air barrier was thickened and irregular (arrow). D. Virus-like particles of 110 nm were seen on both sides of the basal membrane. E. Many endothelial cells contained 60-125 nm viruses in vesicles and free virus-like particles. F. Alveolar spaces (a) were narrowed, and many erythrocytes (e) and macrophages (m) were observed. G, G inset & H. Free viruses of 95-105 nm resided in stromal cells and neighboring myocytes around a blood vessel. The myelin sheath of autonomic nerves was mildly degenerated. A: 5,000X; A inset: 25,000X; B (OM): 50,000X; C: 15,000X; D: 5,000X; D inset left (OM)&right: 30,000X; E left (OM)&right up (OM): 40,000X; E right down (OM): 30,000X; F: 6,000X; G: 12,000X; G inset: 50,000X; H left (OM)&right (OM): 50,000X; I: 10,000X. OM = optically magnified.

DISCUSSION

"Acute-COVID" refers to symptoms lasting up to four weeks, while "Long-COVID" persists beyond four weeks. Long-COVID includes "Subacute-COVID" (>4 to <12 weeks) and "Post-COVID" (>12 weeks without alternative explanation) (National Institute for Health and Care Excellence,2020). 10-20 % of individuals experience Long-COVID, with symptoms lasting up to three months after SARS-CoV-2 infection (World Health Organization, 2023). Severe COVID-19 cases show significant fibrotic changes (Mohammadi *et al*., 2022). SARS and MERS infections have shown pulmonary damage and fibrosis in long-term studies (Ngai *et al*., 2010; Schwensen *et al*., 2021). Likewise, COVID-19 cases can develop pulmonary fibrosis, posing a high risk of respiratory function loss for severe infections (Sheng *et al*., 2020).

In this study, we verified the presence of SARS-CoV-2 virus particles, replicating viruses in vesicles, viral RNA, and spike protein in some of the infected subjects one year after asymptomatic or mild infection. These findings suggest the ability of SARS-CoV-2 to persist in the lungs and raise the possibility of relapsing attacks, akin to tuberculosis. Viruses in vesicles may indicate ongoing viral replication, while free virus-like particles may

represent residual remnants. Despite a low viral load, some long-term lung samples remained positive. The potential for transmissibility should be taken into account and discussed.

After one year, all mild or asymptomatic subjects showed alveolar wall thickening and varying degrees of mild fibrosis, even in PCR-negative lungs. The twelve-month group had a higher fibrosis score than the control group, indicating a potential for post-COVID fibrosis similar to other postviral infections. Unlike symptomatic case reports in the literature, postinfectious bronchiolitis obliterans (PIBO) was not detected in the asymptomatic long-term lungs in our study (Koletsi *et al*., 2021; Lee *et al*., 2022; Yaqoob *et al*., 2022). However, we observed dilated bronchioles with inflammatory cells and mucus, surrounded by peribronchial and perivascular fibrosis, along with interstitial pneumonitis in some short-term groups´ lungs. In some lungs of the twelve-month group, SARS-CoV-2 was detected in Club cells, which play critical roles in both acute and chronic infections and participate in airway epithelium repair (Rokicki *et al*., 2016). They also participate in the repair of the airway epithelium by promoting the development of mesenchymal fibroblasts in conditions such as pulmonary fibrosis and emphysema. When damaged, they are destroyed within 24 hours and regenerated within a month (Weiss, 2014). Despite their regenerative ability, the persistence of SARS-CoV-2 in Club cells can contribute to pathology. In the twelve-month group, electron microscopy revealed alterations in the air-blood barrier components, including thickened basal membranes and folded endothelial cells, similar to fibrosis in interstitial pneumonia (Katzenstein, 1985). The endothelial cells are another component of the air-blood barrier and showed high positivity for SARS-CoV-2 in our study. Myelinated nerves exhibited mild degeneration, which could potentially impact respiratory function.

Macrophages were SARS-CoV-2 positive in some of the subjects after one year of mild or asymptomatic infection. Considering the regeneration capacity and phagocytosis of inflammatory cells, this finding supports continued replication of SARS-CoV-2. A possible chronic lung disease can progress from ongoing infection in asymptomatic patients. In some lungs of the twelve-month group, type II pneumocytes contained SARS-CoV-2, and their surfactant amount was decreased. Various inflammatory pathologies, including interstitial lung disease, are known to cause alteration of surfactant composition and function. A well-functioning surfactant is necessary for normal respiratory function and protection from future infections (Meyer & Zimmerman, 2002).

Most lungs in the eight-day group were positive for mRNA. The patchy immunohistochemical staining pattern, interstitial pneumonia, viruses of sizes ranging from 65 to 110 nm in vesicles and free virus-like particles and the SARS-CoV-2 positive cell types were consistent with the literature on acute SARS-CoV-2 (Zhang *et al*., 2020; Kervancioglu Demirci *et al*., 2023). We observed distinct ultrastructural alterations in long-term asymptomatic lungs, differentiating them from short-term symptomatic lungs (Damiani *et al*., 2021).

Positive nasopharyngeal and sputum samples after recovery from COVID-19 were commonly reported in the literature (Li *et al*., 2020; Yuan *et al*., 2020). Other organs with the potential for viral reservoir, such as residual antigen and RNA of the SARS-CoV-2 virus, have been reported in patients with long COVID following symptomatic initial infection (Goh *et al*., 2022). Some gastrointestinal organs have been found to retain SARS-CoV-2 during the convalescence period (Cheung *et al*., 2022). We previously reported that the corpus cavernosum tested positive one month after recovery from SARS-CoV-2 infection and turned negative after seven months (Kervancioglu Demirci *et al*., 2023). Our heart samples from the eight-day group tested positive for SARS-CoV-2, while those from the twelve-month group were negative. The viral replication in the hearts differed from that in the lungs. The observed high immunopositivity of endothelial cells, as well as the reported positivity in the literature, could be associated with ACE2 receptors present on these cells. Nonetheless, we suggest that transmission and recurrence may occur through viral reservoirs in the lungs.

We detected viral load using qRT-PCR and confirmed the presence of viral particles through electron microscopy. These findings were further validated using immunohistochemistry, which allowed us to observe staining in different cell types. On the other hand, we analyzed a greater number of immunohistochemical samples compared to qRT-PCR samples, resulting in more immunopositive outcomes than qRT-PCR results. In the long-term group, more lungs were immunopositive than with qRT-PCR. This was due to a higher degradation rate of viral RNA. Additionally, we did not provide quantitative data for electron microscopy due to the limited observation area available in electron microscopy. One advantage of our study was the small size of the mice's lungs, allowing us to comprehensively examine the entire lung area through morphological and immunohistochemical analyses using light microscopy. Additionally, this is not a human study, we utilized K18-hACE2 mice, which possess human ACE2 receptors. The subjects were infected once with the virus, kept in a BSL-III facility without reinfection, and did not

have any comorbidities like human subjects. Clinical assessments were conducted following literature guidelines, including regular recording of activity scores and monitoring of weight changes (Moreau *et al*., 2020). We utilized the modified Ashcroft scoring system for a quantitative evaluation of fibrosis, as described in the literature (Hübner *et al*., 2008). However, a limitation of this study was the lack of a scoring system in the literature to directly compare acute and chronic infections. Therefore, we primarily used this scaling for fibrosis scoring in the twelve-month group and to compare it with the control group, providing preliminary data for the eight-day group.

CONCLUSION

In conclusion, this study provides the longest confirmation of SARS-CoV-2 presence in mild and asymptomatic subjects' lungs, emphasizing the residual nature of the virus. Respiratory symptoms and pulmonary function should be monitored for over one year in asymptomatic or mildly infected patients. Some individuals may have replicating or dormant virus in their lungs, raising concerns about unknown severe clinical outcomes. Alveolar septal thickening was observed in all asymptomatic subjects after one year, with potential long-term effects. Persistent viral load, inflammation, and morphological damage can contribute to recurrent infections, post-COVID fibrosis, and chronic lung diseases. The studies conducted previously should be reevaluated in light of our study's findings, and future studies should be designed taking our results into consideration. These results should be corroborated through case reports, clinical studies, and autopsy studies. Patients should be closely monitored in this regard.

ACKNOWLEDGEMENTS

Prof. Dr. Seyhun Solakoglu from the Histology and Embryology Department of Istanbul Faculty of Medicine provided guidance in electron microscopy. Prof. Dr. Mesude Yasemin Özlük from the Pathology Department of Istanbul Faculty of Medicine offered expertise in pathology. Additionally, Prof. Dr. Gülnaz Nural Bekiroglu from the Biostatistics Department of Marmara School of Medicine provided insightful suggestions in statistical analyses.

KERVANCIOGLU DEMIRCI, E.; ONEN, E. A.; YILMAZ, E. S.; MUTLU, H. S. & BINGOL, Z. Cambios histológicos y ultraestructurales en los pulmones un año después de una infección asintomática o leve por SARS-CoV-2: Evaluación del potencial de presencia activa del virus. *Int. J. Morphol., 42(3):*718-727, 2024.

RESUMEN: Investigaciones anteriores sobre COVID-19 o COVID prolongado se centraron principalmente en la presencia de SARS-CoV-2 principalmente en pacientes sintomáticos. Este estudio tuvo como objetivo investigar la persistencia del SARS-CoV-2 después de 1 año de COVID-19 asintomático o leve. Se estudiaron ratones transgénicos K18-hACE2 infectados con SARS-CoV-2 y de control (n=25). Los animales con síntomas moderados y graves se sacrificaron después de ocho días, mientras que los ratones con síntomas leves o asintomáticos se mantuvieron en BSL-III durante doce meses. Los análisis incluyeron estado general, histoquímica, inmunohistoquímica, microscopía electrónica de transmisión y qRT-PCR. Los pulmones del grupo de doce meses mostraron engrosamiento de las paredes alveolares, y algunos pulmones exhibieron reclutamiento de células inflamatorias, presencia de ARNm del SARS-CoV-2, inmunopositividad para la proteína de la espícula del SARS-CoV-2 y TEM mostró virus (60 -125 nm) dentro de las vesículas, lo que indica una replicación continua. Ciertas muestras de pulmón mostraron una presencia persistente de SARS-CoV-2 en exocrinocitos bronquiolares, células endoteliales y macrófagos. El grupo de ocho días presentó neumonitis intersticial viral, inmunopositividad al SARS-CoV-2 y ARNm. Los corazones de ocho días mostraron ARNm viral, mientras que los corazones de doce meses dieron negativo. Algunos animales asintomáticos de doce meses presentaron disminución del surfactante, engrosamiento de la membrana basal, fibrosis y degeneración leve del nervio autónomo. En este estudio realizado en ratones, los hallazgos indican la posibilidad de persistencia crónica del SARS-CoV-2 en los pulmones un año después de la infección inicial leve o asintomática, lo que podría sugerir la posibilidad de episodios recurrentes en condiciones humanas similares. El engrosamiento observado de las paredes alveolares y las posibles áreas fibróticas en estos ratones puede implicar un mayor riesgo de fibrosis post-COVID en humanos. Además, la presencia de células inflamatorias positivas para SARS-CoV-2 en algunos casos murinos asintomáticos podría presagiar una progresión hacia una inflamación continua y una enfermedad pulmonar crónica en humanos. Por lo tanto, se subraya la necesidad de realizar más estudios en seres humanos y realizar un seguimiento atento de las poblaciones humanas de alto riesgo.

PALABRAS CLAVE: Asintomático; Fibrosis; Microscopía electrónica; Síndrome Post-Agudo de COVID-19; Tuberculosis.

REFERENCES

Alp Onen, E.; Sonmez, K.; Yildirim, F.; Demirci, E. K. & Gurel, A. Development, analysis, and preclinical evaluation of inactivated vaccine candidate for prevention of Covid-19 disease. *All Life, 15(1)*:771-93, 2022.

Cheung, C. C. L.; Goh, D.; Lim, X.; Tien, T. Z.; Lim, J. C. T.; Lee, J. N.; Tan, B.; Tay, Z. E. A.; Wan, W. Y.; Chen, E. X.; *et al*. Residual SARS-CoV-2 viral antigens detected in GI and hepatic tissues from five recovered patients with COVID-19. *Gut, 71(1)*:226-9, 2022.

Damiani, S.; Fiorentino, M.; De Palma, A.; Foschini, M. P.; Lazzarotto, T.; Gabrielli, L.; Viale, P. L.; Attard, L.; Riefolo, M. & D'Errico, A. Pathological post-mortem findings in lungs infected with SARS-CoV-2. *J. Pathol., 253(1)*:31-40, 2021.

Goh, D.; Lim, J. C. T.; Fernaíndez, S. B.; Joseph, C. R.; Edwards, S. G.; Neo, Z. W.; Lee, J. N.; Caballero, S. G.; Lau, M. C. & Yeong, J. P. S. Case report: Persistence of residual antigen and RNA of the SARS-CoV-2 virus in tissues of two patients with long COVID. *Front. Immunol., 13*:939989, 2022.

Hübner, R. H.; Gitter, W.; El Mokhtari, N. E.; Mathiak, M.; Both, M.; Bolte, H.; Freitag-Wolf, S. & Bewig, B. Standardized quantification of pulmonary fibrosis in histological samples. *Biotechniques, 44(4)*:507-11, 514-7, 2008.

Katzenstein, A. L. Pathogenesis of "fibrosis" in interstitial pneumonia: an electron microscopic study. *Hum. Pathol., 16(10)*:1015-24, 1985.

Kervancioglu Demirci, E.; Dursun, M.; Seviç, E.; Ergül, R. B.; Önel, M.; Ağˇaçfidan, A. & Kadıogˇlu, A. Evidence for residual SARS-CoV-2 in corpus cavernosum of patients who recovered from COVID-19 infection. *Andrology, 11(6)*:1016-22, 2023.

Koletsi, P.; Antoniadi, M.; Mermiri, D.; Koltsida, G.; Koukou, D.; Noni, M.; Spoulou, V. & Michos, A. A toddler diagnosed with severe postinfectious bronchiolitis obliterans and COVID-19 infection. *Pediatr. Pulmonol., 56(7)*:2381-4, 2021.

Lee, M.; Hwang, J. Y.; Park, S. E.; Jung, S. & Jo, K. J. A case report of postinfectious bronchiolitis obliterans after coronavirus disease 2019 in a 10-year-old child. *J. Korean Med. Sci., 37(31)*:e246, 2022.

Li, Y.; Hu, Y.; Yu, Y.; Zhang, X.; Li, B.; Wu, J.; Li, J.; Wu, Y.; Xia, X.; Tang, H.; *et al*. Positive result of Sars-Cov-2 in faeces and sputum from discharged patients with COVID-19 in Yiwu, China. *J. Med. Virol., 92(10)*:1938-47, 2020.

Merad, M. & Martin, J. C. Pathological inflammation in patients with COVID-19: a key role for monocytes and macrophages. *Nat. Rev. Immunol., 20(6)*:355-62, 2020.

Meyer, K. C. & Zimmerman, J. J. Inflammation and surfactant. *Paediatr. Respir. Rev., 3(4)*:308-14, 2002.

Miesbach, W. Pathological role of angiotensin II in severe COVID-19. *TH Open, 4(2)*:e138-e144, 2020.

Mohammadi, A.; Balan, I.; Yadav, S.; Matos, W. F.; Kharawala, A.; Gaddam, M.; Sarabia, N.; Koneru, S. C.; Suddapalli, S. K. & Marzban, S. Post-COVID-19 pulmonary fibrosis. *Cureus, 14(3)*:e22770, 2022.

Moreau, G. B.; Burgess, S. L.; Sturek, J. M.; Donlan, A. N.; Petri, W. A. & Mann, B. J. Evaluation of K18-hACE2 Mice as a Model of SARS-CoV-2 Infection. *Am. J. Trop. Med. Hyg., 103(3)*:1215-9, 2020.

National Institute for Health and Care Excellence (NICE). *COVID-19 Rapid Guideline: Managing the Long-Term Effects of COVID-19*. London, National Institute for Health and Care Excellence (NICE), 2020.

Ngai, J. C.; Ko, F. W.; Ng, S. S.; To, K. W.; Tong, M. & Hui, D. S. The long-term impact of severe acute respiratory syndrome on pulmonary function, exercise capacity and health status. *Respirology, 15(3)*:543-50, 2010.

Rokicki, W.; Rokicki, M.; Wojtacha, J. & Dzˇeljijli, A. The role and importance of club cells (Clara cells) in the pathogenesis of some respiratory diseases. *Kardiochir. Torakochirurgia Pol., 13(1)*:26-30, 2016.

Schwensen, H. F.; Borreschmidt, L. K.; Storgaard, M.; Redsted, S.; Christensen, S. & Madsen, L. B. Fatal pulmonary fibrosis: a post-COVID-19 autopsy case. *J. Clin. Pathol., 74*:400-2, 2021.

Sheng, G.; Chen, P.; Wei, Y.; Yue, H.; Chu, J.; Zhao, J.; Wang, Y.; Zhang, W. & Zhang, H. L. Viral infection increases the risk of idiopathic pulmonary fibrosis: a meta-analysis. *Chest, 157(5)*:1175-87, 2020.

van Griensven, M.; Dahlweid, F. M.; Giannoudis, P. V.; Wittwer, T.; Böttcher, F.; Breddin, M. & Pape, H. C. Dehydroepiandrosterone (DHEA) modulates the activity and the expression of lymphocyte subpopulations induced by cecal ligation and puncture. *Shock, 18(5)*:445-9, 2002.

Weiss, D. J. Concise review: current status of stem cells and regenerative medicine in lung biology and diseases. *Stem Cells, 32(1)*:16-25, 2014.

World Health Organization. Coronavirus Disease (COVID-19): Post COVID-19 Condition. Geneva, World Health Organization, 2023. Available from: https://www.who.int/news-room/questions-and-answers/item/coronavirus-disease-(covid-19)-post-covid-19-condition

Yaqoob, Z.; Nayef, H. & Alsamman, S. A case of bronchiolitis obliterans developed after mild Covid-19 infection. *Am. J. Respir. Crit. Care Med., 205*:A4210, 2022.

Yuan, B.; Liu, H. Q.; Yang, Z. R.; Chen, Y. X.; Liu, Z. Y.; Zhang, K.; Wang, C.; Li, W. X.; An, Y. W.; Wang, J. C.; *et al*. Recurrence of positive SARS-CoV-2 viral RNA in recovered COVID-19 patients during medical isolation observation. *Sci. Rep., 10(1)*:11887, 2020.

Zhang, H.; Zhou, P.; Wei, Y.; Yue, H.; Wang, Y.; Hu, M.; Zhang, S.; Cao, T.; Yang, C.; Li, M.; *et al*. Histopathologic changes and SARS-CoV-2 immunostaining in the lung of a patient with COVID-19. *Ann. Intern. Med., 172(9)*:629-32, 2020.

Corresponding author:
Assist. Prof. Dr. Elif Kervancioglu Demirci
Histology and Embryology Department
Istanbul Faculty of Medicine
Istanbul University
Fatih 34093
Istanbul
TURKEY

E-mail: elifkervanciogludemirci@istanbul.edu.tr